SUPPLEMENTARY INFORMATION

Identification of Mediator kinase substrates in human cells using cortistatin A and quantitative phosphoproteomics

Zachary C. Poss,[1] Christopher C. Ebmeier,[2] Aaron T. Odell,[2,3] Anupong Tangpeerachaikul,[4] Thomas Lee,[1] Henry E. Pelish,[4] Matthew D. Shair,[4] Robin D. Dowell,[2,3] William M. Old,[2] Dylan J. Taatjes[1]*

1 Department of Chemistry & Biochemistry, University of Colorado, Boulder
2 Department of Molecular, Cell, and Developmental Biology, University of Colorado, Boulder
3 BioFrontiers Institute, University of Colorado, Boulder
4 Department of Chemistry and Chemical Biology, Harvard University

SUPPLEMENTAL NOTE

Rationale for using a 0.1 q-value for identified phosphosites in Table 1

Cortistatin A (CA) appears to be among the most specific CDK inhibitors described to date (Pelish et al., 2015). We observed that the number of phosphosite changes, relative to the whole, was exceedingly small (75/12000: less than 1% of the sites decrease at all). Therefore, we feel justified in loosening the adjusted p-value, especially considering that this is a discovery-based experiment.

Thresholding based on the q-value (p-value corrected for multiple testing by controlling the false-discovery rate by the Benjamini-Hochberg method (Benjamini and Hochberg, 1995)) represents a trade-off between accepted false-positives (e.g. phosphopeptides with extreme ratios that are not actually changing with CA) and false-negatives (e.g. phosphopeptides that are actually changing, but with ratios not rising to the required level of significance). The choice of what adjusted p-value is used, whether 0.05 or 0.1 in this case, represents different choices with respect to this tradeoff. The FDR thresholds of 0.05 and 0.1 yield 45 and 76 ratios accepted as changing, respectively. This translates to an estimated number of accepted false-positive ratios for these two thresholds of 2.2 and 7.6, respectively. We regard the difference in 2.2 vs. 7.6 false-positives an acceptable tradeoff for the increased number of true positives resulting from the statistical power. Because this is a discovery experiment for CDK8/19 substrates, which are largely unreported, we relaxed the FDR due to the fact that this results in only about 5 extra false positives by chance. Since we also report the adjusted p-value (q-value) for all of the CDK8/19-dependent phosphorylation changes, readers are free to decide if such a value is too large to justify biological follow-up.

SUPPLEMENTAL FIGURE LEGENDS

Figure S1, related to Table 1. Motif, pathway, and protein interaction analyses of Mediator kinase substrates

(A) Motif analysis of CDK8/19 substrates using iceLogo. Peptides of the same length were input and centered on the phosphorylated residue.

(B) GO biological process (BP), molecular function (MF) and cellular compartment (CC) completed with DAVID (Huang da et al., 2009) using proteins from **Table 1**. Enriched terms (p-value and FDR ≤ 0.05) are shown.

(C) Protein interaction analysis of CDK8/19 substrates (**Table 1**) using the STRING database (high confidence interactions, ≥ 0.7). Nodes represent proteins and lines between them represent a documented interaction.

Figure S2, related to Figure 3. Treatment of HCT116 cells with the kinase inhibitors RO-3306 (CDK1) and SP600125 (JNK)

(A) Western blot examining the SIRT1 pT530 signal in the presence of increasing amounts of RO-3306, SP600125, or both inhibitors together. As CDK1 and JNK1 have been reported to phosphorylate this site,

we tested whether we could detect this change using the SIRT1 pT530 phosphoantibody. No large change was detected, even with both inhibitors used together.
(B) Western blot using high concentrations of both RO-3306 and SP600125 in the presence of increasing amounts of CA. When CA was added to the cells, we were able to again detect a decrease in the pT530 signal for SIRT1, supporting CDK8/19 as kinases that phosphorylate this site.

Figure S3, related to Figure 4. Overlap of gene expression changes between stable knockdown of CDK8 or CDK19 and 3h or 24h CA treatment in HCT116 cells.
(A and B) Genes whose expression increased or decreased with stable knockdown of either CDK8 (A) or CDK19 (B) compared to cells treated with CA for 3h. Comparison is between microarray data (Galbraith et al., 2013) using stable CDK8/19 knockdown (shRNA) vs. CA treatment in HCT116 cells under normal growth conditions.
(C) Genes that show increased expression upon CA treatment (3h) or CDK8 or CDK19 knockdown.
(D and E) Genes whose expression increased or decreased with stable knockdown of either CDK8 (D) or CDK19 (E) compared to cells treated with CA for 24h. Note that the overlap between stable knockdowns and kinase inhibition at 24h remains modest. Comparison is between microarray data (Galbraith et al., 2013) using stable CDK8/19 knockdown (shRNA) vs. CA treatment in HCT116 cells under normal growth conditions.
(F) Hypergeometric test between Mediator kinase targets and factors whose Transfac matrices were over-represented in promoters of genes differentially expressed with 3h CA treatment. The p-value suggests that the likelihood of observing this amount of overlap by chance is low.

Figure S4, related to Figure 4. Functional links between Mediator kinase targets and gene expression changes
TFBS analysis of promoters for genes whose expression changed with 3h CA treatment (listed in **Figure 4A**). Promoters (±2kb from the TSS of the canonical isoform) were analyzed using the F-Match tool. Overrepresented sites with at least a 1.5-fold increase relative to control promoters are shown for Transfac vertebrate matrices, with the matrix name on the left side of the heat map. The 'NA' and its corresponding color on the heat map refers to a particular matrix not being identified as overrepresented. Highlighted at far left in **BLACK FONT** are selected Transfac matrices. In **RED FONT** are examples of Mediator kinase targets that are either represented by the Transfac matrix or are known co-regulators of the TF(s) representing that matrix.

A

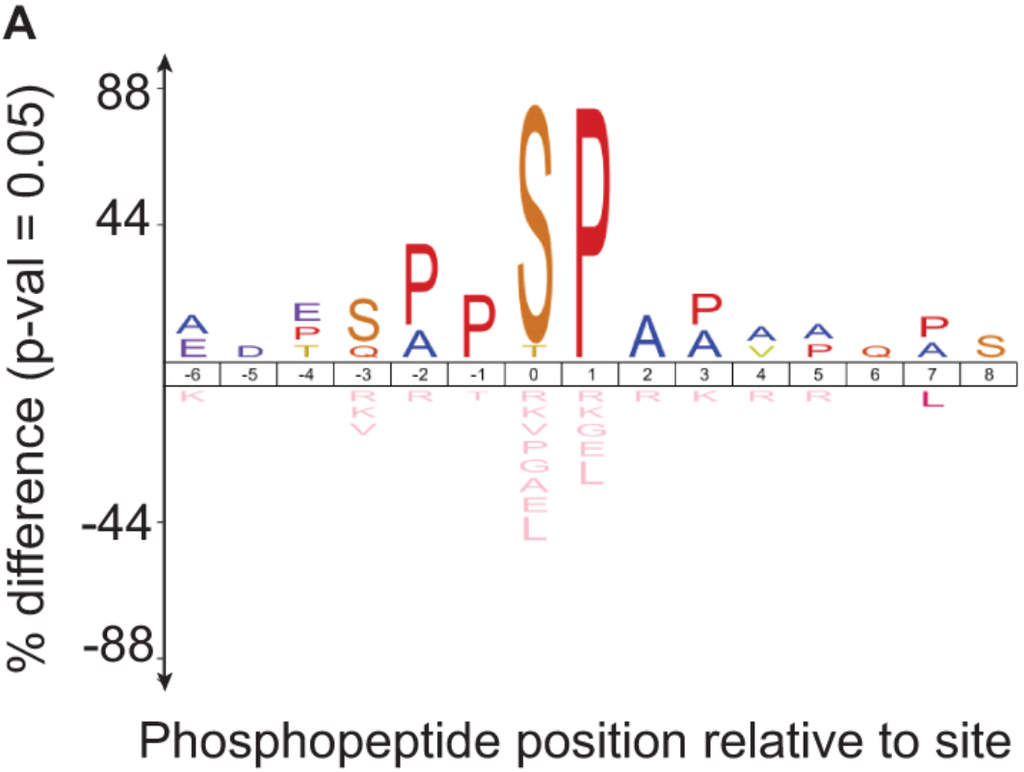
% difference (p-val = 0.05)
88
44
-44
-88
-6
-5
-4
-3
-2
-1
0
1
2
3
4
5
6
7
8
Phosphopeptide position relative to site

B

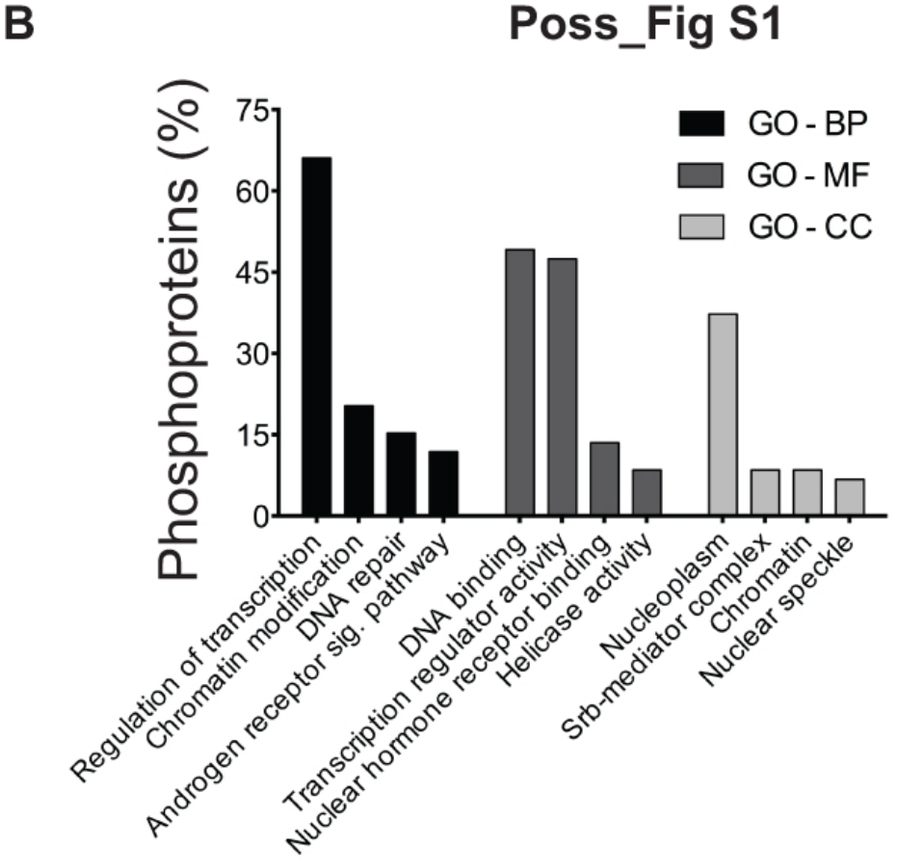
Phosphoproteins (%)
75
60
45
30
15
0
GO - BP
GO - MF
GO - CC
Regulation of transcription
Chromatin modification
DNA repair
Androgen receptor sig. pathway
DNA binding
Transcription regulator activity
Nuclear hormone receptor binding
Helicase activity
Nucleoplasm
Srb-mediator complex
Chromatin
Nuclear speckle

C

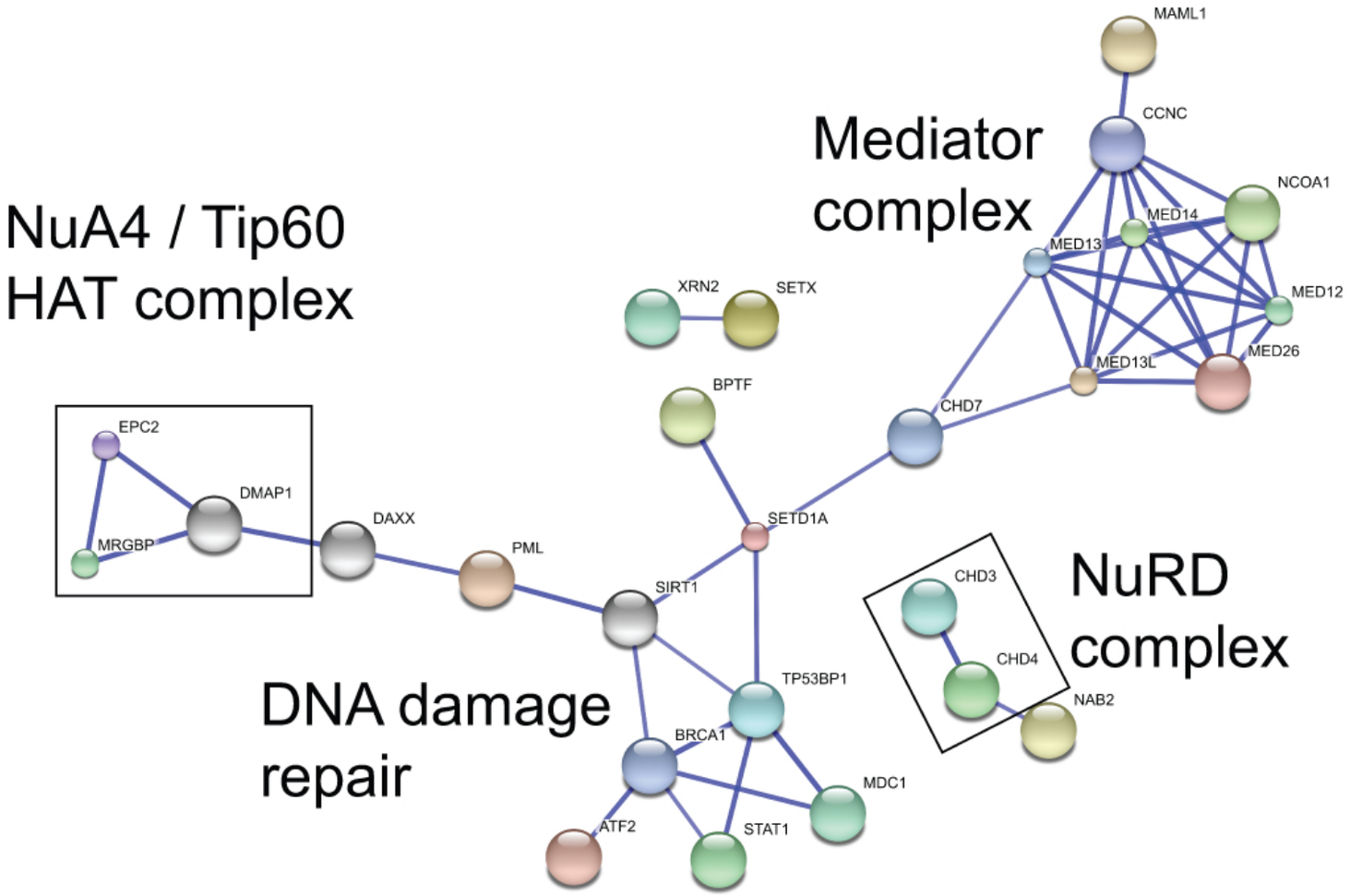
NuA4 / Tip60
HAT complex
Mediator
complex
NuRD
complex
DNA damage
repair
MAML1
CCNC
NCOA1
MED14
MED13
MED12
MED26
MED13L
CHD7
XRN2
SETX
BPTF
EPC2
DMAP1
MRGBP
DAXX
PML
SETD1A
SIRT1
CHD3
CHD4
NAB2
TP53BP1
BRCA1
MDC1
ATF2
STAT1

A

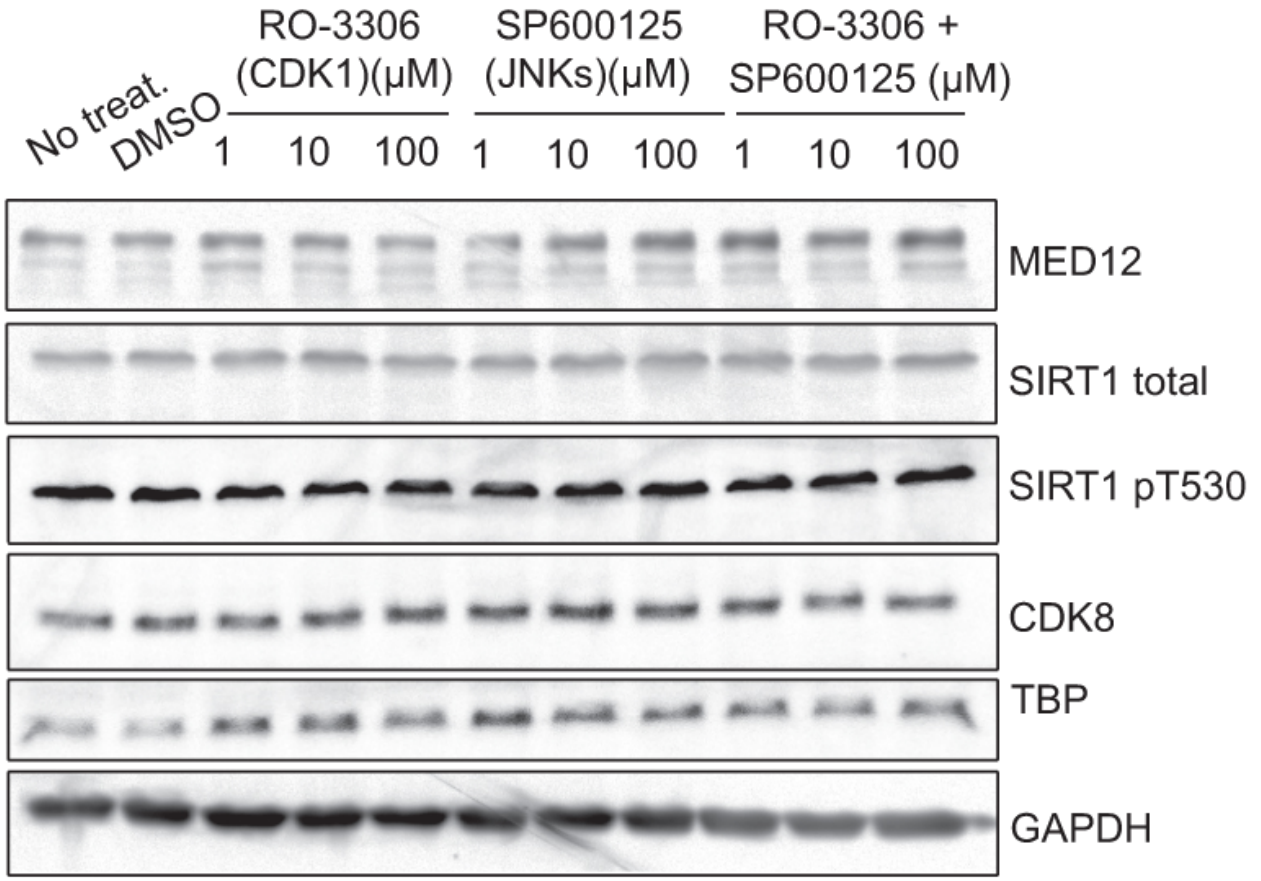

western blot - HCT116

B

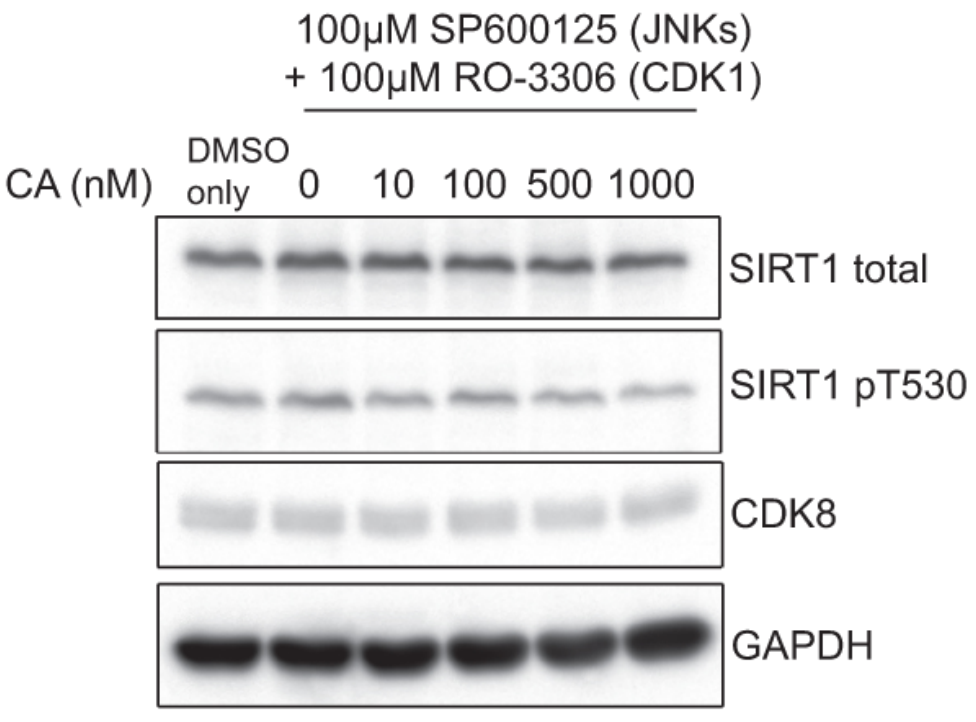

western blot - HCT116

A

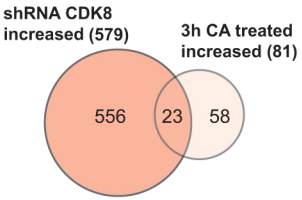

Gene	shRNA FC	shRNA p-value	CA FC	CA p-value
EHF	17.97	8.37E-08	1.28	4.44E-02
SOCS6	1.77	1.57E-04	1.31	3.44E-02
VSNL1	30.80	2.09E-09	1.32	1.74E-02
MSX1	1.94	1.56E-04	1.33	1.31E-02
NT5DC3	1.78	1.66E-05	1.33	1.31E-02
HTR7	1.82	2.05E-04	1.34	4.08E-02
ZBED2	10.22	2.60E-09	1.34	7.76E-03
HES1	1.67	2.81E-05	1.35	1.31E-02
RND3	1.96	7.73E-04	1.35	7.76E-03
HOXB8	2.10	2.27E-07	1.39	7.76E-03
KLF4	2.19	4.48E-06	1.42	7.76E-03
SEMA3C	2.98	4.63E-06	1.42	7.76E-03
GATA2	2.18	1.12E-05	1.43	7.76E-03
KLF11	1.55	2.87E-04	1.45	7.76E-03
SIX1	1.50	2.47E-05	1.45	7.76E-03
BHLHE40	1.69	5.26E-04	1.52	7.76E-03
TRIML2	1.64	5.24E-04	1.54	7.76E-03
SLC16A6	4.15	1.51E-07	1.54	1.31E-02
ARL4C	5.74	6.05E-06	1.61	7.76E-03
ITGB8	3.32	2.01E-06	1.74	7.76E-03
TNFSF18	62.43	7.64E-08	1.75	1.31E-02
KRT80	2.98	3.09E-06	1.81	7.76E-03
ID3	1.62	7.17E-05	1.85	7.76E-03

B

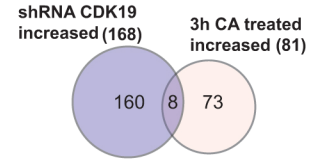

Gene	shRNA FC	shRNA p-value	CA FC	CA p-value
EHF	21.87	5.65E-08	1.28	4.44E-02
ZNF827	1.67	2.28E-06	1.31	3.44E-02
VSNL1	37.07	1.52E-09	1.32	1.74E-02
HOXB8	2.36	9.22E-08	1.39	7.76E-03
KLF11	1.68	1.13E-04	1.45	7.76E-03
SPRY1	1.82	1.00E-06	1.52	7.76E-03
SLC16A6	3.87	2.04E-07	1.54	1.31E-02
ITGB8	2.32	1.61E-05	1.74	7.76E-03

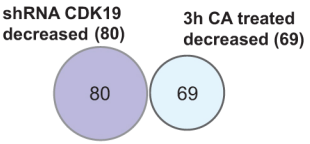

D

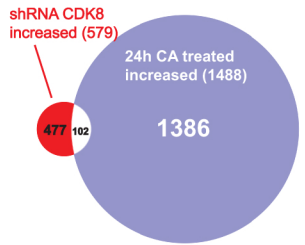

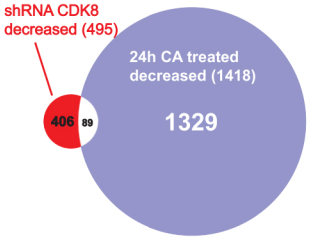

E

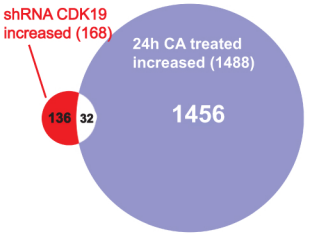

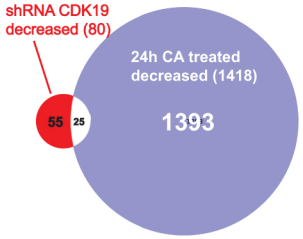

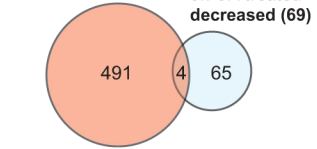

Gene	shRNA FC	shRNA p-value	CA FC	CA p-value
EGR1	0.37	7.65E-06	0.23	7.76E-03
NFATC2	0.53	1.66E-07	0.70	2.60E-02
OR51B4	0.63	1.04E-05	0.73	2.16E-02
ZNF165	0.63	1.03E-04	0.76	4.44E-02

C

Incr. genes dependent on both CDK8/19 activity

Gene	shCDK8 FC	shCDK19 FC	CA FC
EHF	17.97	21.87	1.28
VSNL1	30.80	37.07	1.32
HOXB8	2.10	2.36	1.39
KLF11	1.55	1.68	1.45
SLC16A6	4.15	3.87	1.54
ITGB8	3.32	2.32	1.74

F

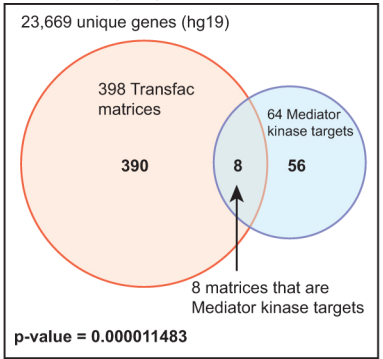

Poss_Figure S4

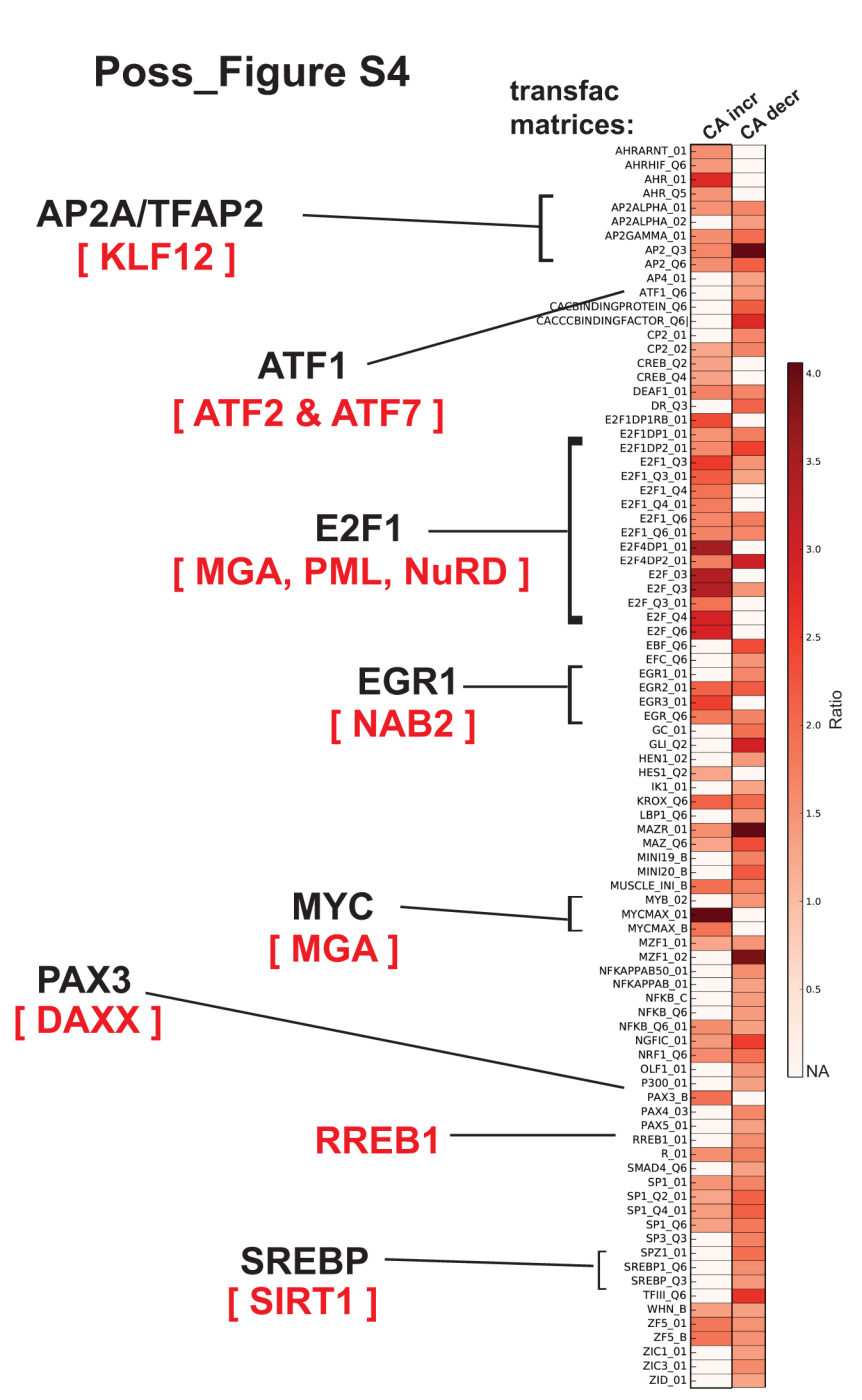

SUPPLEMENTAL TABLES

Table S1, related to Figure 1. All phosphosites quantified in the CA treatment phosphoproteomic screen
Table shows the entire Phospho (STY) output from a Maxquant search that was processed in Perseus in the following manner: reverse and contaminant reads were removed, the ratios for the label swap experiment were inverted, the site table was expanded, and only quantified sites were kept. "H/L norm 1-3" represent biological triplicate CA treatment phosphoproteomic experiments in HCT116 cells. "PEP" and "Score" are posterior error probability and Andromeda score, respectively. The "seq window" shows peptides centered on the phosphosite, while the "modified seq" shows modifications in parentheses.

Table S2, related to Table 1. All high confidence phosphosites that change with CA treatment in HCT116 cells
Phosphosites that were quantified in two or more biological replicates and have an empirical Bayes adjusted p-value <0.1 for 1hr CA treatment are shown. This table includes phosphosites that both increase and decrease with CA treatment. H/L ratios for the protein containing the phosphosite are also shown to exclude the possibility that a given phosphosite changes with CA treatment due to a protein-level change. If a protein ratio is bolded and italicized, the protein-level ratio was not quantified in the 1hr treatment condition, but was quantified at another time point. 'NaN' indicates that no protein-level ratio was calculated, and 'Not found' indicates that the protein was not identified in the proteome analysis.

Table S3, related to Figure 4. All gene expression data (RNA-Seq; 3h or 24h, ± CA)

Table S4, related to Figure 5. All quantified proteins from CA treatment time course in HCT116 cells
This is a simplified version of the proteinGroups file from a Maxquant search of biological duplicate experiments in which HCT116 cells were treated with CA across a time series. Cells were treated with 100nM CA (heavy media) at 0h, 1h, 3h, 6h, 18h, and 24h and compared with untreated controls (DMSO, light media). Cell populations at the 0h time point were each DMSO treated. 'Protein IDs' represents all Uniprot accession matches for a given protein.

Table S5, related to Figure 5. Empirical Bayes analysis of CA-dependent proteome changes
Values for 18h and 24h replicates are $\log_2$ transformations of H/L ratios from SILAC experiments. "AveExpr" is the mean of the 18h and 24h $\log_2$ values. "F" is the value for the F-statistic comparing late treatments to t0. "PValue" and "adjPVal" are the result of an empirical Bayes analysis.

Table S6, related to Figure 5D. GSEA analysis of time series proteomics data for HCT116 cells treated with CA
Shown are pages for each time point of treatment (0, 1, 3, 6, 18, 24h), starting with t = 0, with normalized enrichment scores (NES), FDR values, and gene names that comprise the hallmark.

Table S7, related to Figure 4. IPA upstream regulator analysis for CA-dependent gene expression changes
Factors with a listed value in the z-score column were deemed significant by IPA.

Table S8, related to Figure 2 & 4. Mediator kinase targets linked to the TFs β-catenin or E2F1
List of high-confidence Mediator kinase substrates with functional links to β-catenin or E2F1 function or target gene expression. The putative mechanisms by which the factors listed affect β-catenin or E2F1 target gene expression are varied and may either positively or negatively affect transcription. As one example, the ATF2 and ATF7 TFs can effectively act as surrogates for β-catenin, at least in some contexts. In hematopoietic cells, ATF2 and ATF7 can activate TCF/LEF function in the absence of β-catenin (Grumolato et al., 2013). We identified four high-confidence phosphorylation sites on ATF2 + ATF7; whereas these do not appear to affect ATF2 or ATF7 stability, interactions with TCF/LEF or other DNA-bound proteins may be controlled by phosphorylation at these sites. As another example, SIRT1 is a key chromatin and metabolic regulator that can deacetylate histones, TFs, and metabolic enzymes. A SIRT1 phosphorylation site, T530, identified here as a CDK8/19 substrate, is known to activate the deacetylase

activity of SIRT1 (Sasaki et al., 2008). In colon cancer cells, it has been shown that SIRT1 de-acetylates β-catenin, which negatively affects target gene expression by promoting β-catenin export to the cytoplasm (Firestein et al., 2008). Consequently, blocking CDK8/CDK19-dependent SIRT1 T530 phosphorylation with CA would be expected to increase expression of some β-catenin target genes. In agreement, we find that MYC, BHLEH40, FGFBP1, and other β-catenin target genes show increased expression in CA-treated HCT116 cells.

SUPPLEMENTAL EXPERIMENTAL PROCEDURES

Phosphoproteomics sample preparation

Cells were passaged 7-8 times in SILAC media on 15cm dishes. For each replicate, approximately 20mg total protein was harvested for analysis after treatment with either 100nM CA or DMSO for 1 hr. For one replicate, treatment conditions were reversed and light cells were CA treated and heavy cells were DMSO treated. To harvest, media was removed and each dish was scraped in 750μl 95°C SDT (4% SDS, 100mM Tris pH 7.9, 10mM TCEP) buffer with subsequent heating at 95°C for 10 min. Lysates were sonicated for 1-2 minutes each. Protein concentrations were determined using a BCA assay and samples were mixed 1:1 based on total protein concentrations. FASP was carried out in two 10kDa MWCO filters with a 50mM iodoacetamide alkylation step and proteins were digested in 2M urea with 2% wt/wt Lys-C (Wako) for 6 h and 2% modified trypsin (Promega) for 12 h at 37°C. FASP eluates were acidified and desalted on Oasis HLB extraction cartridges.

Phosphoproteomics and quantitative proteomics data analysis

All raw MS files for phosphoproteomics and quantative proteomics were searched using the MaxQuant (v1.4.1.2) software package. Triplicate phosphoproteomic and duplicate proteomic treatments with a CA-time course were searched individually against the Uniprot human proteome database (downloaded on 1/27/2014) using the default MaxQuant parameters, except: multiplicity was set to 2 (heavy/light) with Arg10 and Lys8 selected, LysC/P was selected as an additional enzyme, "re-quantify" was unchecked, and Phospho (STY) was selected as a variable modification in both runs. For phosphosite analysis, the Phospho (STY) table was processed with Perseus (v1.4.1.3) using the following workflow: reverse and contaminant reads were removed, the site table was expanded to accommodate differentially phosphorylated peptides, and rows without any quantification were removed after site table expansion. For protein quantification with a CA treatment time course, the protein Groups table was processed similarly to the Phospho (STY) table, except that there was no need for expansion of the site table.

In vitro kinase assays

For validation of GST-tagged substrates identified in the phosphoproteomics experiments, the assay was done as described (Bancerek et al., 2013), except that the total reaction volume was reduced to 10μl and samples were loaded on a pre-cast, 4-20% gradient gel (BioRad) and coomassie stained for loading control analysis. For CDK8 module kinase assays using SIRT1 as a substrate, His-SIRT1 (addgene 13735) was purified as described (Hallows et al., 2006) except that no eluate dialysis was performed, and assays were carried out using 1X PK buffer (NEB) with 100μM cold ATP at 30°C for the indicated time. Reaction mixes were created such that each sample on the gel corresponded to 0.25μl CDK8 module and 25ng of SIRT1. Phosphorylation of SIRT1 T530 was detected using western blotting on a 4-20% precast gradient gel. Assays were done as previously described for the CDK1, ERK2, and GSK3β kinase assays. Purified CDK1-Cyclin B and GSK3β were purchased from New England Biolabs (NEB) and Abcam, respectively. Phosphorylated ERK2 was a gift from the laboratory of Natalie Ahn.

RNA-Seq

HCT116 cells were treated with either 100nM CA or DMSO for 3h (n=3) and 24h (n=3). Cells were washed twice with cold PBS and scraped into TRIzol reagent (Life Technologies). After harvesting, the RNA was further purified using an RNeasy mini kit (Qiagen) with on-column DNase I digestion. Libraries for Illumina sequencing were generated via the Illumina TruSEQ stranded mRNA prep kit. Samples were run in a

single lane on an Illumina HiSEQ 2000 sequencer with a single read flow cell using 1x 50bp reads and a 6-cycle index read. Reads were mapped to the hg19 reference genome using Tophat2 v.2.0.6 with custom settings. HTSeq v.9.6.1 was used to obtain read counts over annotated genes and differentially expressed genes were called using Cufflinks v.2.1.1.

STRING and Gene Ontology (GO) analyses

High confidence phosphosites identified as CDK8/19 substrates were submitted to the STRING database with human as the selected organism and the "multiple names" option. The confidence score was set to high (≥ 0.7). GO analyses were completed using the DAVID bioinformatics tool.

Hypergeometic test for Mediator kinase targets and Transfac matrices

To perform the hypergeometric test we assumed that Mediator kinase target proteins (64) could be represented by any gene annotated in hg19 (23,669). Using all Transfac matrices available in the public database (398), we identified 8 binding sites of high confidence Mediator kinase targets, with a probability that this event could occur at random of 0.000011483.

HCT116 compound treatment for immunoblotting, and antibodies

HCT116 cells were grown in 6cm dishes to approximately 80% confluency and were treated with either DMSO or CA at 10, 50, 100, 500, 1000nM for 2h. Cells were harvested by scraping, whole-cell extracts were made using RIPA buffer, and protein amounts were quantified using a BCA assay. 30μg total protein was loaded in each lane, and the following antibodies were used: MED12 (Bethyl A300-774A, 1:2000), Total SIRT1 (Santa Cruz sc-15404, 1:3000), SIRT1 T530 Phospho (Abcam ab156585, 1:1000), CCNC (Santa Cruz sc-1061, 1:1000), CDK8 (Santa Cruz sc-1521, 1:1000), and TBP (Santa Cruz sc-273, 1:1000).

For evaluation of STAT1 S727 phosphorylation upon IFN gamma treatment with and without CA, HCT116 cells were grown in the same manner as described previously. Cells were pre-treated with either DMSO or increasing concentrations of CA for 45m, and then treated with IFN-γ (eBioscience) at a final concentration of 10ng/ml for 45m. Cells were washed with cold PBS containing protease and phosphatase inhibitors, scraped in PBS, and spun at 2000 rpm for 5m at 4°C. Cold RIPA buffer containing protease and phosphatase inhibitors was used to resuspend the cell pellets, and lysates were nutated at 4°C for 15m and subsequently sonicated in a cold water bath. Sonicated lysates were spun at 14,000 rpm at 4°C and 30μg cleared RIPA lysates were used for western blot analysis.

For treatment with RO-3306 and SP600125, cells were incubated in the presence of the indicated concentration of compound with or without CA for 2.5h. Cells were subsequently harvested and extracts were made according to above.

Autophosphorylation of CDK8 module and TiO_2 enrichment

Approximately 200pmol of CDK8 module (CDK8, CCNC, MED12 and MED13) was expressed and purified as described (Knuesel et al., 2009) and incubated with 1mM ATP in 1x PK buffer (NEB) at 37°C for 2h. Total protein was TCA precipitated and the protein pellet was resuspended in 50μl SDT buffer. The sample was heated for 5 min at 95°C to completely solubilize the pellet, diluted in UA buffer, and small-scale FASP was carried out in a 30kDa MWCO filter (Amicon, 500μl capacity). Protein was digested to peptides with both 2% Lys-C (6h) and trypsin (12h) wt/wt at room temperature. Samples were desalted on C18 spin columns (Pierce), acidified, and titanium dioxide enrichment of phosphopeptides was carried out with a 10:1 wt/wt ratio. Samples were subjected to 1D LC/MS/MS on an Orbitrap LTQ (Thermo Fisher). Raw files were searched with MaxQuant.

Transcription factor binding site (TFBS) analysis

Promoters for differentially expressed genes were extracted from UCSC Genome Browser and promoter analysis (+/-2kb from the TSS) was conducted with F-Match, a part of the Transfac public database. Only vertebrate Transfac matrices were selected for the output. Control promoters were taken from genes in the HCT116 dataset whose expression was unaffected with CA treatment.

SUPPLEMENTAL REFERENCES

Alves-Guerra, M.C., Ronchini, C., and Capobianco, A.J. (2007). Mastermind-like 1 Is a specific coactivator of beta-catenin transcription activation and is essential for colon carcinoma cell survival. Cancer Res *67*, 8690-8698.

Bancerek, J., Poss, Z.C., Steinparzer, I., Sedlyarov, V., Pfaffenwimmer, T., Mikulic, I., Dolken, L., Strobl, B., Muller, M., Taatjes, D.J.*, et al.* (2013). CDK8 Kinase Phosphorylates Transcription Factor STAT1 to Selectively Regulate the Interferon Response. Immunity *38*, 250-262.

Benjamini, Y., and Hochberg, Y. (1995). Controlling the False Discovery Rate: a Practical and Powerful Approach to Multiple Testing. J R Statist Soc B. *57*, 289-300.

Carrera, I., Janody, F., Leeds, N., Duveau, F., and Treisman, J.E. (2008). Pygopus activates Wingless target gene transcription through the mediator complex subunits Med12 and Med13. Proc Natl Acad Sci U S A *105*, 6644-6649.

Chen, J., Luo, Q., Yuan, Y., Huang, X., Cai, W., Li, C., Wei, T., Zhang, L., Yang, M., Liu, Q.*, et al.* (2010). Pygo2 associates with MLL2 histone methyltransferase and GCN5 histone acetyltransferase complexes to augment Wnt target gene expression and breast cancer stem-like cell expansion. Mol Cell Biol *30*, 5621-5635.

Chen, Z., and Han, M. (2001). C. elegans Rb, NuRD, and Ras regulate lin-39-mediated cell fusion during vulval fate specification. Current biology : CB *11*, 1874-1879.

de la Roche, M., Worm, J., and Bienz, M. (2008). The function of BCL9 in Wnt/beta-catenin signaling and colorectal cancer cells. BMC Cancer *8*, 199.

Firestein, R., Blander, G., Michan, S., Oberdoerffer, P., Ogino, S., Campbell, J., Bhimavarapu, A., Luikenhuis, S., de Cabo, R., Fuchs, C.*, et al.* (2008). The SIRT1 deacetylase suppresses intestinal tumorigenesis and colon cancer growth. PLoS One *3*, e2020.

Grumolato, L., Liu, G., Haremaki, T., Mungamuri, S.K., Mong, P., Akiri, G., Lopez-Bergami, P., Arita, A., Anouar, Y., Mlodzik, M.*, et al.* (2013). beta-Catenin-independent activation of TCF1/LEF1 in human hematopoietic tumor cells through interaction with ATF2 transcription factors. PLoS genetics *9*, e1003603.

Hallows, W.C., Lee, S., and Denu, J.M. (2006). Sirtuins deacetylate and activate mammalian acetyl-CoA synthetases. Proc Natl Acad Sci U S A *103*, 10230-10235.

Huang da, W., Sherman, B.T., and Lempicki, R.A. (2009). Systematic and integrative analysis of large gene lists using DAVID bioinformatics resources. Nature protocols *4*, 44-57.

Kim, S., Xu, X., Hecht, A., and Boyer, T.G. (2006). Mediator is a transducer of Wnt/beta-catenin signaling. J. Biol. Chem. *281*, 14066-14075.

Knuesel, M.T., Meyer, K.D., Donner, A.J., Espinosa, J.M., and Taatjes, D.J. (2009). The human CDK8 subcomplex is a histone kinase that requires Med12 for activity and can function independently of Mediator. Mol Cell Biol *29*, 650-661.

Kramps, T., Peter, O., Brunner, E., Nellen, D., Froesch, B., Chatterjee, S., Murone, M., Zullig, S., and Basler, K. (2002). Wnt/wingless signaling requires BCL9/legless-mediated recruitment of pygopus to the nuclear beta-catenin-TCF complex. Cell *109*, 47-60.

Mahmoudi, T., Boj, S.F., Hatzis, P., Li, V.S., Taouatas, N., Vries, R.G., Teunissen, H., Begthel, H., Korving, J., Mohammed, S.*, et al.* (2010). The leukemia-associated Mllt10/Af10-Dot1l are Tcf4/beta-catenin coactivators essential for intestinal homeostasis. PLoS biology *8*, e1000539.

Mohan, M., Herz, H.M., Takahashi, Y.H., Lin, C., Lai, K.C., Zhang, Y., Washburn, M.P., Florens, L., and Shilatifard, A. (2010). Linking H3K79 trimethylation to Wnt signaling through a novel Dot1-containing complex (DotCom). Genes Dev *24*, 574-589.

Ogawa, H., Ishiguro, K., Gaubatz, S., Livingston, D.M., and Nakatani, Y. (2002). A complex with chromatin modifiers that occupies E2F- and Myc-responsive genes in G0 cells. Science *296*, 1132-1136.

Pelish, H.E., Liau, B.B., Nitulescu, II, Tangpeerachaikul, A., Poss, Z.C., Da Silva, D.H., Caruso, B.T., Arefolov, A., Fadeyi, O., Christie, A.L.*, et al.* (2015). Mediator kinase inhibition further activates super-enhancer-associated genes in AML. Nature *526*, 273-276.

Salz, T., Li, G., Kaye, F., Zhou, L., Qiu, Y., and Huang, S. (2014). hSETD1A regulates Wnt target genes and controls tumor growth of colorectal cancer cells. Cancer Res *74*, 775-786.

Sasaki, T., Maier, B., Koclega, K.D., Chruszcz, M., Gluba, W., Stukenberg, P.T., Minor, W., and Scrable, H. (2008). Phosphorylation regulates SIRT1 function. PLoS One *3*, e4020.

Shtutman, M., Zhurinsky, J., Oren, M., Levina, E., and Ben-Ze'ev, A. (2002). PML is a target gene of beta-catenin and plakoglobin, and coactivates beta-catenin-mediated transcription. Cancer Res *62*, 5947-5954.

Sierra, J., Yoshida, T., Joazeiro, C.A., and Jones, K.A. (2006). The APC tumor suppressor counteracts beta-catenin activation and H3K4 methylation at Wnt target genes. Genes Dev *20*, 586-600.
Sustmann, C., Flach, H., Ebert, H., Eastman, Q., and Grosschedl, R. (2008). Cell-type-specific function of BCL9 involves a transcriptional activation domain that synergizes with beta-catenin. Mol Cell Biol *28*, 3526-3537.
Talluri, S., and Dick, F.A. (2014). The retinoblastoma protein and PML collaborate to organize heterochromatin and silence E2F-responsive genes during senescence. Cell Cycle *13*, 641-651.
Vernier, M., Bourdeau, V., Gaumont-Leclerc, M.F., Moiseeva, O., Begin, V., Saad, F., Mes-Masson, A.M., and Ferbeyre, G. (2011). Regulation of E2Fs and senescence by PML nuclear bodies. Genes Dev *25*, 41-50.
Zhang, M., Mahoney, E., Zuo, T., Manchanda, P.K., Davuluri, R.V., and Kirschner, L.S. (2014). Protein kinase A activation enhances beta-catenin transcriptional activity through nuclear localization to PML bodies. PLoS One *9*, e109523.